Inclusive Hard Diffraction at HERA

Alexander Proskuryakov

Moscow State University, Leninskie gory, Moscow 119991, Russia

(On behalf of the H1 and ZEUS Collaborations)

Recent data from the H1 and ZEUS experiments on hard inclusive diffraction are discussed. Results of QCD analyses of the diffractive deep-inelastic scattering processes are reported. Predictions based on the extracted parton densities are compared to diffractive dijet measurements.

1 Introduction

One of the most interesting results obtained at HERA is the observation that a significant amount of events in deep-inelastic scattering (DIS) is of diffractive nature. Diffractive processes are usually described in Regge theory [1] as the exchange of a trajectory with the vacuum quantum numbers, the Pomeron trajectory. However, the observation of jets in diffractive $\bar{p}p$ scattering [2] opened the possibility to study diffraction in the framework of quantum chromodynamics (QCD). Diffractive reactions in DIS provide additional information on the structure of diffraction offering an opportunity to study the transition from soft to hard diffraction. The concept of diffractive parton distribution functions (DPDFs) plays an important role in the study of diffractive reactions in DIS and is essential input to calculations of hard diffractive processes at the LHC.

This paper briefly reports recent results on hard inclusive diffraction from the H1 and ZEUS experiments.

2 Kinematics and Cross Sections

Fig. 1 shows a schematic diagram for the diffractive process $ep \to eXp$. The data used for the

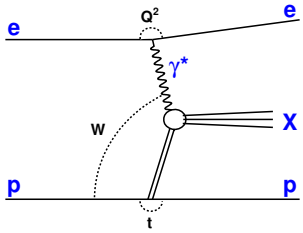

Figure 1: Schematic diagram for the reaction $ep \to eXp$.

measurements reported in the paper were collected at HERA ep collider, when HERA collided

positron (electron) of 27.5 GeV with protons of 920 GeV. The kinematics of the diffractive reaction $ep \to eXp$ is described by the following variables:

- $Q^2 = -(p_e - p_{e'})^2$, the negative four-momentum squared of the virtual photon, where $p_e(p_{e'})$ is the four-momentum the incident (scattered) electron;
- $W^2 = (p_\gamma + p_p)^2$, the squared centre-of-mass energy of the photon-proton system, where p_γ and p_p are the four-momenta of the virtual photon and the incident proton respectively;
- $M_X^2 = (p_\gamma + p_p - p_{p'})^2$, the squared mass of the system X, where $p_{p'}$ is the four-momentum of the scattered proton;
- $t = (p_p - p_{p'})^2$, the squared four-momentum transfer at the proton vertex;
- y=$(p_\gamma \cdot p_p)/(p_e \cdot p_p)$, the fraction of the electron energy transferred to the proton in the proton rest frame.

The two dimensionless variables x_{IP} and β often used instead of W and M_X are defined as $x_{IP} = (p_p - p_{p'}) \cdot p_\gamma / p_p \cdot p_\gamma$ and $\beta = Q^2/2(p_p - p_{p'}) \cdot p_\gamma$.

The cross section for the diffractive process $ep \to eXp$ can be expressed in terms of the diffractive reduced cross section $\sigma_r^{D(4)}(\beta, Q^2, x_{ip}, t)$:

$$\frac{d\sigma^{ep}}{dx_{IP} d\beta dQ^2 dt} = \frac{4\pi\alpha^2}{\beta Q^4}(1 - y + \frac{y^2}{2})\sigma_r^{D(4)},$$

where $\sigma_r^{D(4)}$ depends on the diffractive structure functions $F_2^{D(4)}$ and $F_L^{D(4)}$ as

$$\sigma_r^{D(4)} = F_2^{D(4)} - \frac{y^2}{2(1 - y + y^2/2)} F_L^{D(4)}.$$

The diffractive structure function $F_2^{D(3)}(\beta, Q^2, x_{IP})$ and the reduced cross section $\sigma_r^{D(3)}(\beta, Q^2, x_{IP})$ are obtained by integrating $F_2^{D(4)}(\beta, Q^2, x_{IP}, t)$ and $\sigma_r^{D(4)}(\beta, Q^2, x_{IP}, t)$ over t.

3 Selection of Diffractive Events

At HERA, diffractive events were selected either by the detection of the final state proton [3, 4] or on the basis of a large rapidity gap between the system X and the outgoing proton [4, 5]. The diffractive contribution was also identified by the M_X method [6] based on the shape of the mass distribution of the system X.

In the methods based on the large rapidity gap (LRG) or M_X selections the measured cross section includes a contribution from events of the type $ep \to eXN$, in which the proton dissociates into a low mass state N. The contribution from these proton-dissociative events is estimated from a Monte Carlo simulation.

The method based on the final state proton detection does not have background from proton-dissociative events. It allows a direct measurement of the variable t and gives access to higher values of x_{IP}. However, the statistical precision is limited by the acceptance of the proton taggers.

Within the normalisation uncertainties the results from the different methods agree reasonably well [4].

4 Results

4.1 t Dependence

The differential cross section $d\sigma/dt$ for the diffractive reaction $ep \to eXp$ is well approximated by the exponential function $e^{-b|t|}$. The differential cross section in the kinematic range $0.0002 < x_{IP} < 0.01$ and $0.01 < x_{IP} < 0.1$ is presented in Fig. 2. The value of the slope parameter b obtained from the fit to the data is $b = 6 - 7$ GeV^{-2} [3, 4].

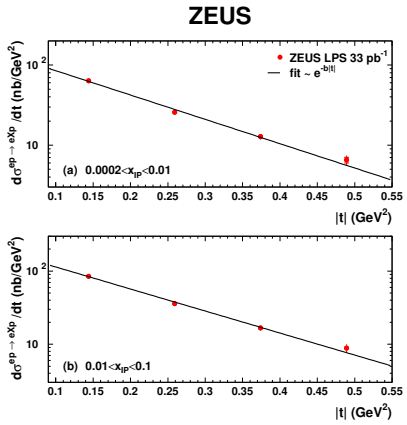

Figure 2: The differential cross section $d\sigma/dt$ for for (a) $0.0002 < x_{IP} < 0.01$ and (b) $0.01 < x_{IP} < 0.1$.

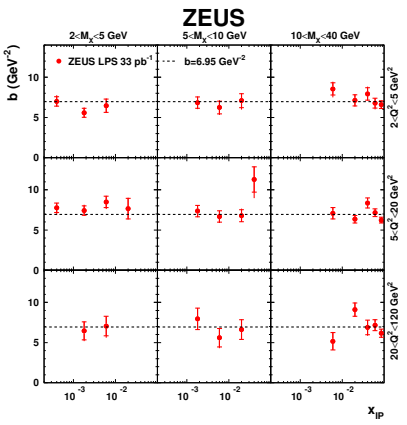

Figure 3: The value of the exponential-slope parameter b of the differential cross section $d\sigma^{ep\to eXp}/dt \propto e^{-b|t|}$ as a function of x_{IP} in bins of Q^2 and M_X.

The values of the slope parameter b in different bins of x_{IP}, Q^2 and M_X are shown in Fig. 3. The shape of the t distribution does not depend on x_{IP}, Q^2 and M_X.

4.2 x_{IP} Dependence

In the framework of Regge phenomenology the x_{IP} dependence of the diffractive structure functions is related to the parameters of the Pomeron trajectory parameterised as $\alpha_{IP}(t) = \alpha_{IP}(0) + \alpha'_{IP}t$. The Pomeron intercept, $\alpha_{IP}(0)$, in soft hadronic interactions is $1.096^{+0.012}_{-0.09}$ [7]. However, the same parameter is significantly larger in the diffractive production of heavy vector mesons [9]. The slope of the Pomeron trajectory, α'_{IP} was found to be 0.25 GeV^{-2} [8]. The parameters of the Pomeron trajectory can also be determined from the measurements of the diffractive reaction $ep \to eXp$.

Fig. 4 shows the reduced cross section $\sigma_r^{D(4)}$ in two t bins, $0.09 < |t| < 0.19$ GeV^2 and $0.19 < |t| < 0.55$ GeV^2. The data presented in the figure were fitted to the form

$$F_2^{D(4)} = f_{IP}(x_{IP}, t) \cdot F_2^{IP}(\beta, Q^2) + n_R \cdot f_R(x_{IP}, t) \cdot F_2^R(\beta, Q^2)$$

where n_R is a normalisation term. It was assumed that $F_2^{D(4)} = \sigma_r^{D(4)}$ and the fit was limited to $y < 0.5$ to reduce the influence of F_L^D. The Pomeron and Reggeon fluxes were parameterised

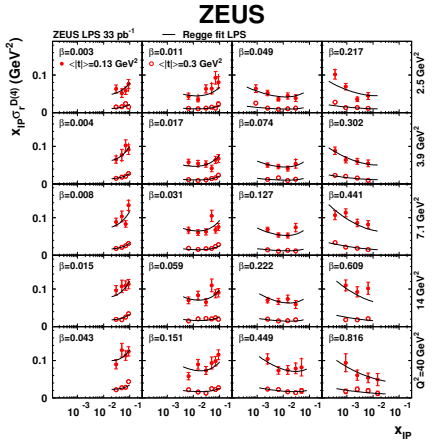

Figure 4: The reduced diffractive cross section multiplied by x_{IP}, $x_{IP}\sigma_r^{D(4)}$, in two t bins as a function of x_{IP} for different values of Q^2 and β.

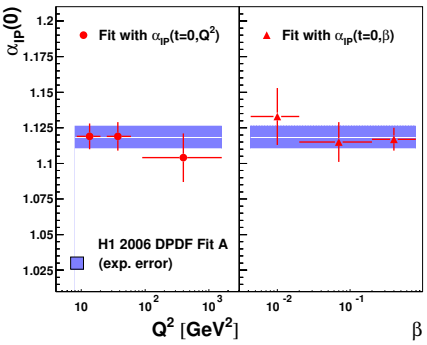

Figure 5: The Pomeron intercept $\alpha_{IP}(0)$ as a function of Q^2 and β.

as [1]

$$f_{IP,R}(x_{IP},t) = \frac{e^{B_{IP,R}t}}{x_{IP}^{2\alpha_{IP,R}(t)-1}},$$

with linear trajectories $\alpha_{IP,R}(t) = \alpha_{IP,R}(0) + \alpha'_{IP,R}t$. The Reggeon structure function, F_2^R, was taken to be equal to the pion structure function as parameterised by GRV [10, 11, 12]. The resulting Pomeron intercept is $\alpha_{IP}(0) = 1.11 \pm 0.02(\text{stat.})^{+0.01}_{-0.02}(\text{syst.}) \pm 0.02(\text{model})$. The slope of the Pomeron trajectory is $\alpha'_{IP} = -0.01 \pm 0.06(\text{stat.})^{+0.04}_{-0.08}(\text{syst.}) \pm 0.04(\text{model})$ GeV^{-2}.

Similar fits were performed to the LRG data [4, 5]. Fig. 5 shows the values of $\alpha_{IP}(0)$ as a function of Q^2 and β. The present data do not exhibit a significant dependence on Q^2 and β.

4.3 QCD Analysis of Diffractive Data

A QCD analysis of diffractive data is based on the QCD factorisation theorem [13, 14, 15, 16]. The theorem allows to express the diffractive structure functions $F_{2/L}^{D(3}$ as a convolution of coefficient functions and DPDFs:

$$F_{2/L}^{D(3)}(\beta, Q^2, x_{IP}) = \sum_i \int_\beta^1 \frac{dz}{z} C_{2/L,i}(\frac{\beta}{z}) f_i^D(z, x_{IP}, Q^2),$$

where the sum runs over partons of type i and z is the momentum fraction of the parton, entering the hard subprocess. The coefficient functions $C_{2/L,i}$ are the same as in inclusive DIS. The DPDFs $f_i^D(z, x_{IP}, Q^2)$ are densities of partons of type i with fractional momentum zx_{IP} in a proton.

The x_{IP} dependence of the DPDFs is parameterised as a sum of two contributions, separately factorisable into a term depending on x_{IP} and a term depending on z and Q^2,

$$f_i^D(z, x_{IP}, Q^2) = f_{IP}(x_{IP}) f_i^{IP}(z, Q^2) + f_R(x_{IP}) f_i^R(z, Q^2).$$

This assumption of proton vertex factorisation is a good approximation for the data used in this analysis [4, 5]. The flux factors f_{IP} and f_R describing the x_{IP} dependence of the Pomeron and Reggeon contributions were parameterised using Regge theory. The DPDFs were parameterised at the starting scale Q_0^2 in term of quark singlet and gluon distributions as $zf(z,Q_0^2) = Az^B(1-z)^C$. The parameters describing the quarks and gluons at the starting scale were fitted to the data using NLO DGLAP [17, 18, 19] evolution to all values of Q^2.

The DPDFs have been extracted in several different analyses [5, 20, 21]. It was shown that the gluon distribution obtained in the fits to the inclusive data only has a large uncertainty at high z.

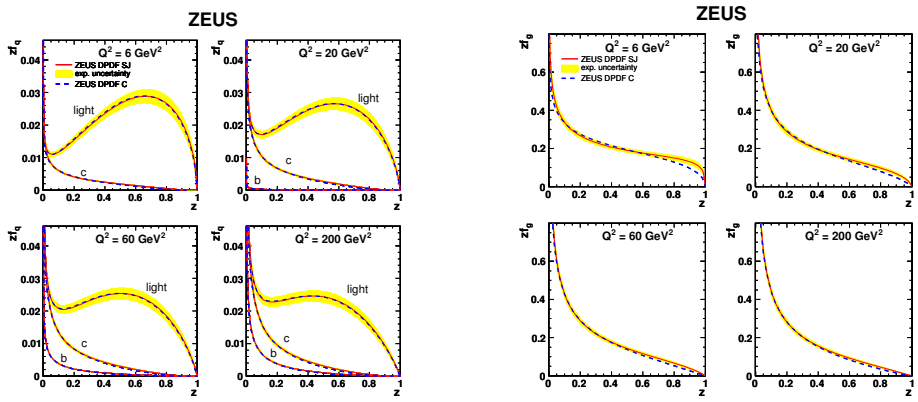

Figure 6: The quark(left plot) and gluon(right plot) distributions obtained from fit to the ZEUS inclusive and dijet data for four different values of Q^2. The shaded error bands show the experimental uncertainty.

The inclusion of the diffractive DIS dijet cross sections in the fit provides an additional constraint on the gluon, allowing the determination of the gluon density with better accuracy [21, 22]. The quark and gluon densities from the fit to the ZEUS inclusive and dijet data are shown with their experimental uncertainties for $Q^2 = 6, 20, 60$ and 200 GeV^2 in Fig. 6. The fraction of the momentum of the diffractive exchange carried by the gluons is $(60-70)\%$ [21, 22].

4.4 Diffractive Dijet Photoproduction

The QCD factorisation theorem does not hold in hadron-hadron collisions. The same can be expected in the dijet photoproduction process where the photon can behave as a hadron-like particle at low x_γ, the fraction of the photon energy invested in producing the dijet system.

Fig. 7 shows the dijet photoproduction cross section as a function of x_γ together with the NLO QCD predictions based on several DPDFs and photon PDFs parameterisations.

The results from the ZEUS experiment are consistent with the NLO QCD predictions. The H1 experiment observes a suppression of NLO QCD predictions by factor 0.5 at all values of x_γ.

The disagreement can be explained by the different kinematic regions used in both experiments. The ZEUS analysis selected jets with higher transverse energies. The new measurements of the dijet photoproduction cross section performed by the H1 experiment [23] indicates that the suppression factor can depend on the transverse energy of the selected jets.

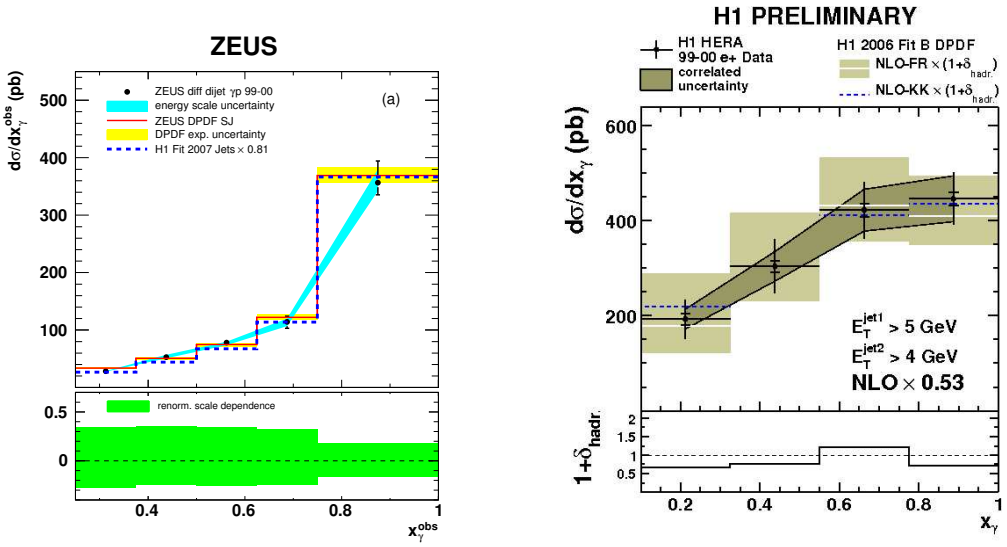

Figure 7: The differential cross section for the diffractive photoproduction of dijets as a function of x_γ as measured by ZEUS (left plot) and H1 (right plot). NLO QCD predictions for several DPDFs parameterisations are also shown (scaled by a factor of 0.53 on the right plot). The shaded bands show the uncertainty resulting from the variation of the renormalisation scale.

4.5 Longitudinal Diffractive Structure Function

The first measurement of the longitudinal structure function F_L^D [24] performed by the H1 experiment is presented in Fig. 8. The analysis is based on the data samples with different proton beam energies of 460, 575 and 920 GeV. The results are compatible with the predictions from the QCD fits to the previous inclusive data.

5 Conclusions

Recent results from HERA provided a lot on new information on diffraction. The cross sections of the diffractive reaction $ep \to eXp$ have been measured in a very wide range of Q^2, W and M_X. Different methods used to select diffractive processes give consistent results. Diffractive data have been used in QCD analyses and the diffractive parton density functions have been determined. The extracted diffractive parton density functions describes the diffractive charm and dijet production. They are an important input for calculation of the hard diffractive processes at the LHC.

Acknowledgements

It is a pleasure to thank the organisers for this stimulating and enjoyable workshop.

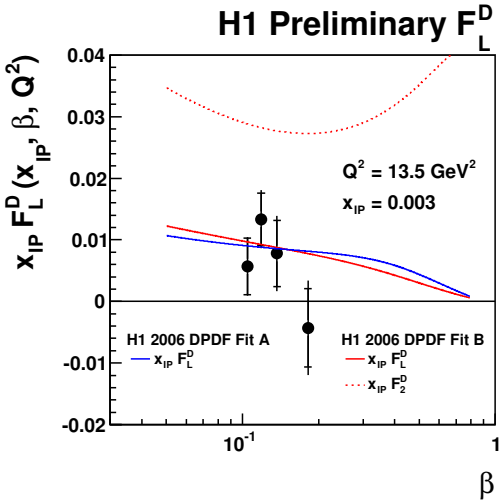

Figure 8: The diffractive longitudinal structure function F_L^D multiplied by x_{IP} as a function of β. The predictions from NLO QCD fits are also shown.

References

[1] P.D.B. Collins, An Introduction to Regge Theory and High Energy Physics, Cambridge University Press, Cambridge (1977). Cambridge University Press, Cambridge.

[2] UA8 Coll., A. Brandt et al., Phys. Lett. **B297** 417 (1992).

[3] H1 Coll., A. Aktas et al., Eur. Phys. J. **C48** 749 (2006).

[4] ZEUS Coll., S. Chekanov et al., Nucl. Phys.**B816** 1 (2009).

[5] H1 Coll., A. Aktas et al., Eur. Phys. J. **C48** 715 (2006).

[6] ZEUS Coll., S. Chekanov et al., Nucl. Phys.**B800** 1 (2008).

[7] J.-R. Cudell, K. Kang and S.K. Kim, Phys.Lett. **B395** 311 (1997).

[8] V. Barone and E. Pedazzi, High-Energy Particle Diffraction,Springer Verlag, Heidelberg (2002).

[9] H. Abramowicz, Int. J. Mod. Phys. **A15 S1b** 495 (2000).

[10] M. Glück, E. Reya and A. Vogt, Z. Phys. **C53** 127 (1992)

[11] M. Glück, E. Reya and A. Vogt, Z. Phys. **C53** 651 (1992)

[12] M. Glück, E. Reya and A. Vogt, Z. Phys. **C67** 433 (1995)

[13] J.C. Collins, Phys. Rev. **D57** 3051 (1998).

[14] Erratum, ibid **D61** 019902 (2000).

[15] L. Trentadue and G. Veneziano, Phys. Lett **D323** 201 (1994).

[16] A. Berera and D.E. Soper, Phys. Rev. **D53** 6162 (1996).

[17] V.N. Gribov and L.N. Lipatov, Sov. J. Nucl, Phys. **15** 438 (1972).

[18] Yu.L. Dokshitzer, Sov. Phy. JETP **46** 641 (1977).

[19] G. Altarelli and G. Parisi, Nucl. Phys. **B126** 298 (1977).

[20] A.D. Martin, M.G. Ryskin and G. Watt, Phys. Lett. **B644** 311 (2007).

[21] H1 Coll., A. Aktas et al., JHEP **0710:042** (2007).

[22] ZEUS Coll., to be published.

[23] K. Cerny, Dijets in diffractive photoproduction, in XVI International Workshop on Deep Inelastic Scattering, DIS 2008. April 2008, London

[24] H1 Coll., to be published.